ACS Photonics

Letter

pubs.acs.org/journal/apchd5

Plasmonic Nanostars as Efficient Broadband Scatterers for Random Lasing

Johannes Ziegler,* Christian Wörister, Cynthia Vidal, Calin Hrelescu, and Thomas A. Klar

Institute of Applied Physics, Johannes Kepler University Linz, 4040 Linz, Austria

Supporting Information

ABSTRACT: Huge spectral coverage of random lasing throughout the visible up to the infrared range is achieved with star-shaped gold nanoparticles ("nanostars"). As intrinsically broadband scattering centers, the nanostars are suspended in solutions of various laser dyes, forming randomly arranged resonators which support coherent laser modes. The narrow emission line widths of 0.13 nm or below suggest that gold nanostars provide an efficient coherent feedback for random lasers over an extensive range of wavelengths, all together spanning almost a full optical octave from yellow to infrared.

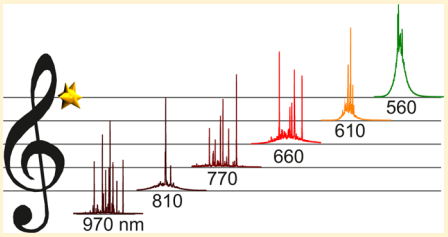

KEYWORDS: *random lasing, gold nanostars, plasmon resonances, multiple scattering, gain*

Considerable experimental research interest was initiated by early reports of lasers with mirrorless feedback due to scattering.[1,2] Incoherent light amplification, which basically is amplified spontaneous emission (ASE), was obtained in diffusive media with gain,[3] as well as coherent random lasing.[4,5]

Resonant random lasing is realized by randomly formed closed-loop cavities[6−9] of dielectric or metallic nanostructures inside a gain medium. This permits cheap and easy fabrication of random lasers, in contrast to conventional lasers, which require accurate fabrication and extremely precise alignment of the resonator. Thus, random lasers are attractive for a manifold of potential applications, ranging from smart imaging[10] and medical diagnostics,[11−14] to lighting devices and displays.[15]

Organic dye solutions[16] as gain material and noble metal nanoparticles (NPs) as scattering centers is a supremely fascinating combination, since such NPs exhibit localized surface plasmon resonances in the visible and near-infrared spectral range. The resonances allow more efficient scattering of light than in case of dielectric NPs of similar dimensions, made out of high refractive index dielectrics such as TiO_2 or ZnO. Moreover, plasmonic resonances induce highly confined and strongly enhanced optical fields near the NPs' surface and change the local density of optical states in the close vicinity of the NPs. Thereby, the radiative and nonradiative transition rates of nearby dye molecules are modified by plasmonic NPs.[17,18] The spectral position of the plasmon resonances is strongly linked to shape, material, and environment of the NPs, which has evoked manifold types of plasmonic NPs. Complex-shaped ones, such as gold nanostars, already turned out to be beneficial in many aspects.[19−23] Their strongly enhanced electric fields are highly localized at the spiky tips,[24−26] and the associated plasmonic hotspots effectively augment interactions with nearby molecules.[27] For an efficient interaction of NPs and dye molecules in random lasers, the plasmon resonances need to spectrally overlap the emission of the desired active medium. The emission itself is required, in addition, to be spectrally well separated from the absorption spectrum to avoid reabsorption, which counteracts gain. Improvements of ASE[28] and random lasing due to plasmonic effects have been established with round NPs of gold,[29−32] otherwise, chiefly with silver NPs.[33,34] Yet, scattering of such NPs is restricted alone to the short-wavelength part of the visible spectrum. In contrast, especially biological applications demand radiation in the biological transparency window in the near-infrared (700−1000 nm), limited to few commercial long-wavelength fluorescent dyes, which commonly suffer low absorption and poor photostability. Ways to circumvent the low absorption and increase the separation between excitation and laser emission have been explored using energy transfer systems.[35−37] An expanded wavelength range of random lasing with plasmonic NPs, however, has not yet been demonstrated and would bridge the gap between UV[4,38] and infrared[39−41] random lasers.

In this Letter, we accomplish random lasing from yellow up to the infrared range with plasmonic gold nanostars suspended in a variety of laser dyes. We hereby exploit the superiority of the complex-shaped nanostars over conventionally shaped NPs as scattering centers in random lasers.[42] When we illuminate a defined area of suspensions containing nanostars and gain, we observe the appearance of narrow line width peaks in the emission spectra over more than 410 nm. The spectral width of the peaks is as narrow as 0.13 nm (the resolution limit of the spectrometer in use) and obviously origins from coherently lasing modes. The nanostars can randomly form resonant cavities in the gain medium, while their broadband scattering spectra due to multiple plasmon resonances[24] provide sufficient spectral overlap with the emission of the laser dyes. Together with the huge field enhancements at their spiky tips (see, for example, Figure 3 in ref 24 and Figures 4 and 5 in ref 26), this

Received: February 17, 2016
Published: May 20, 2016

DOI: 10.1021/acsphotonics.6b00111
ACS Photonics 2016, 3, 919−923

facilitates efficient random lasing and enables the broad spectral coverage of narrow line width emission, even under a fixed excitation wavelength of 532 nm.

The studied random lasers comprised suspensions of gain medium and gold nanostars. The nanostars were wet-chemically synthesized with a seed-mediated growth method[43] and the particle concentration was increased by gentle centrifugation and redispersion in deionized water. Figure 1a displays scanning electron microscope images of the gold nanostars, showcasing their spiky tips. An ensemble extinction spectrum in aqueous solution and a dark-field scattering spectrum of a single exemplary gold nanostar are presented in Figure 1b. It can be clearly seen that each nanostar features an intrinsically broadband scattering spectrum essentially originating from multiple plasmon resonances.[24] Calculated scattering and absorption cross sections of a representative gold nanostar are provided in the Supporting Information, Figure S1. The extinction of the ensemble up to about 550 nm is primarily attributed to the d-band absorption of gold, whereas the extinction due to plasmon resonances reaches up to infrared wavelengths. A variety of commercially available laser dyes[44] was utilized as gain media. Rhodamine 6G, rhodamine B, rhodamine 101, DCM, pyridine 1, pyridine 2, styryl 8, rhodamine 800, styryl 9M, styryl 15, IR 140, and styryl 14 were dissolved with typical concentrations in the millimolar range, complying with their solubility and the respective absorption cross section at 532 nm. Each dye solution was mixed with a stock solution of nanostars which served as multiple scattering centers for random lasing. The detailed parameters for the various dyes are listed in Table 1. The suspensions were then filled into quartz cuvettes (inner dimensions 10 mm × 2 mm) with four transparent windows to perform the random lasing measurements.

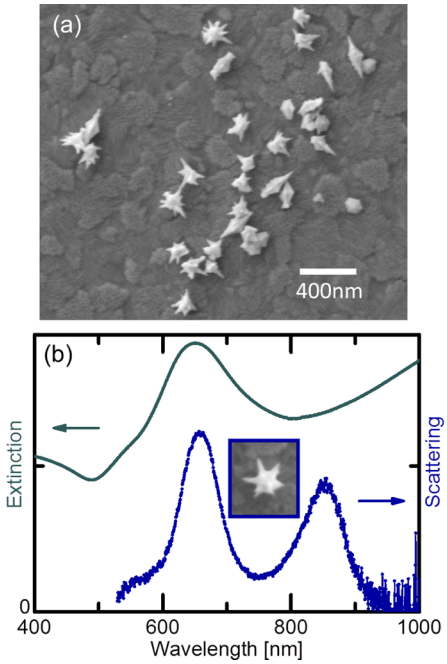

Figure 1. (a) Electron micrograph presents gold nanostars with spiky tips. (b) Ensemble extinction spectrum (olive curve) of nanostars in aqueous solution and dark-field scattering spectrum (blue curve) of a single nanostar show intrinsic broadband scattering throughout the visible up to the infrared spectral range.

The experimental setup featured stripe-like illumination of the cuvettes with side detection. A diode-pumped, passively Q-switched solid state laser (CryLaS GmbH, pulse length shorter than 1.3 ns, maximal pulse energy 20 μJ) was used to excite the suspensions with single pulses at a wavelength of 532 nm. The excitation beam was shaped into a thin stripe by two crossed cylindrical lenses and focused in the plane of two razor blades. In order to establish a 3 mm long, 55 μm wide excitation stripe on the suspensions, the razor blades selected the homogeneous central part of the beam. It was projected onto the cuvette by an imaging lens to reduce Fresnel diffraction and to ensure a constant pump fluence of up to 7 mJ/cm^2 along the stripe. The cuvette was slightly tilted to avoid optical feedback from the cuvette walls. The rim of the excitation stripe was positioned close to the side window for detection, as illustrated by the illumination and detection geometry in Figure 2a, such that there was no unpumped region between the illuminated volume and the exit window. The emission from the pumped excitation volume was coupled out of the side window and focused onto the entrance slit of a spectrometer (Newport MS260i) equipped with a Peltier-cooled charge-coupled device

Table 1. Experimental Parameters of the Suspensions for Random Lasing[a]

dye	solvent	concn of stock solution (mM)	absorption cross section at 532 nm (10^{-16} cm^2)	added stock solution of nanostars (%)	applied pump fluence (mJ/cm^2)
rhodamine 6G	ethanol	1	3.8	30	7.0
rhodamine B	methanol	2	1.6	13	0.6
rhodamine 101	ethanol	5	0.88	13	0.4
DCM	ethanol	6	0.51	13	7.0
DCM	DMSO	2	0.51	13	4
pyridine 1	ethanol	1	0.82	13	2
pyridine 2	ethanol	2	1.3	30	2
styryl 8	DMSO	5	1.9	13	0.3
rhodamine 800	DMSO	10	0.13	13	7
styryl 9M	DMSO	5	1.5	13	0.1
styryl 15	DMSO	5	0.64	13	0.4
IR 140	DMSO	5	0.19	13	3
styryl 14	DMSO	5	1.5	13	0.6

[a]Absorption cross sections are estimated from extinction curves of ref 44 by σ (532 nm) = 1000 ln10 ε (532 nm)/N_A.

DOI: 10.1021/acsphotonics.6b00111
ACS Photonics 2016, 3, 919−923

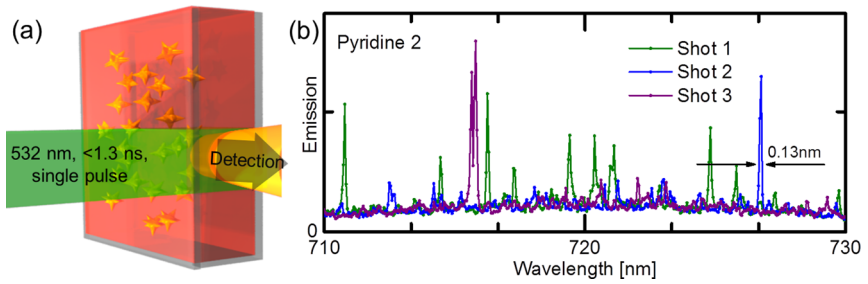

Figure 2. (a) Illustration of the stripe illumination and the detection from the edge of the cuvette. (b) Emission properties of a solution containing gold nanostars as scattering centers and pyridine 2 as gain medium. Single excitation pulses above threshold provoke random lasing with spectrally narrow peaks. The spectral position of the peaks varies for consecutive pulses due to the rearrangement of the nanostars in the gain region of the solution.

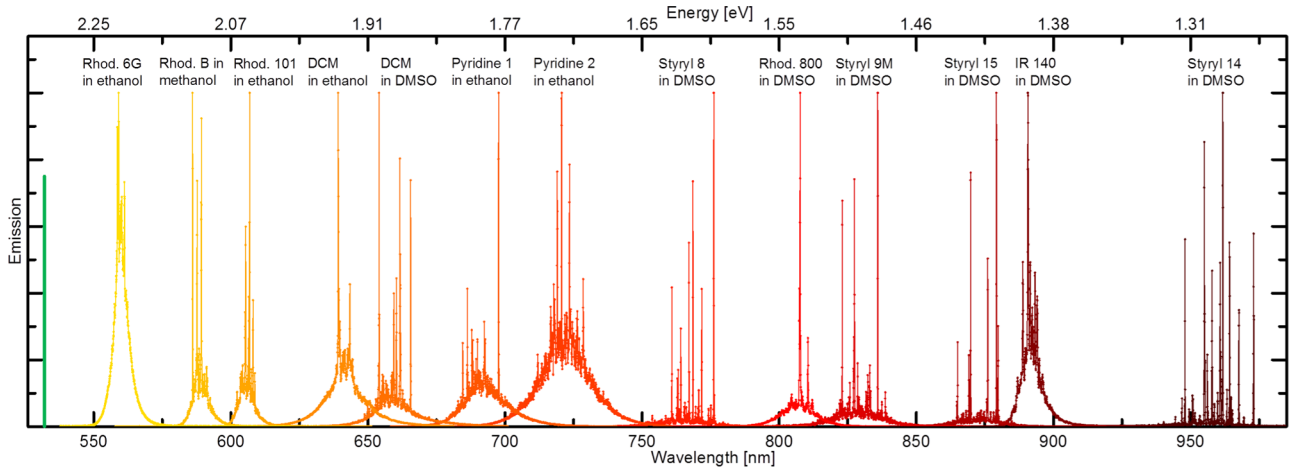

Figure 3. Emission of a series of dyes in random lasers containing gold nanostars. The tunability spans almost a full optical octave. Single-pulsed excitation at a wavelength of 532 nm was employed with fluences above the specific lasing threshold. Narrow line width peaks emerge for all studied dyes, indicating coherent random lasing.

camera (Andor iVac). A 532 nm notch filter was used when necessary to suppress the detection of scattered excitation light.

Figure 2b exemplifies the single-shot emission characteristics of random lasing for a solution containing the laser dye pyridine 2 and gold nanostars. Pyridine 2 in ethanol offers a large Stokes shift, providing substantial absorption at the wavelength of excitation and a broad gain spectrum around 720 nm. The absorption cross sections for pyridine 2 and each subsequently studied laser dye are given in Table 1. The three curves in Figure 2b represent emission spectra recorded for consecutive excitation pulses well above threshold. Several spectrally narrow features arise out of the broad fluorescence background, symptomatic for coherent multimode random lasing. The nanostars efficiently scatter photons emitted by the pyridine 2 molecules and, hence, grant the necessary feedback mechanism. Moreover, the high local fields may provide an additional excitation enhancement of the molecules, which can cause a significant increase in the effective emission.[18,45] The measured spectral width of the peaks reaches down to 0.13 nm, which constitutes the resolution of the spectrometer (grating 1200 lines/mm, entrance slit 20 μm). The values therefore represent an upper limit and the actual line widths of the lasing modes might be well below. The random arrangement of nanostars in the gain region of the solution changes from shot to shot (spaced by 1 s) due to Brownian motion and is not fixed as in a polymer matrix. Therefore, the closed-loop resonator cavities of the random laser alter for each single-pulsed excitation, leading to variation in spectral position, number, and intensities of the peaks, as shown by the variations in the three curves of Figure 2b.

Next, we investigated how random lasing over a wide spectral range can be achieved by the combination of nanostars and various laser dyes. Figure 3 displays the emission of a series of dyes incorporated in the random lasers. Each dye is excited with single pump pulses at a wavelength of 532 nm with the fluences indicated in Table 1, above the specific thresholds for random lasing. In the short-wavelength part of the spectrum, a mixture of gold nanostars and the widely established and routinely deployed dye rhodamine 6G exhibits random lasing centered around 560 nm. Single lasing peaks are clearly observable in the spectrum. This is also the case for other rhodamines such as rhodamine B, which emits around 590 nm, and rhodamine 101 emitting around 610 nm. Furthermore, DCM in ethanol features random lasing centered at 640 nm, while DCM in DMSO lases at 660 nm. Pyridines 1 and 2 in ethanol show lasing modes around 690 and 720 nm, respectively. Moving on to the "deep red" part of the spectrum, random lasing occurs around 770 nm for styryl 8 in DMSO and around 810 nm for rhodamine 800. Styryl 9M and styryl 15 manifest multiple lasing modes, emerging out of a broad gain spectrum centered around 830 and 870 nm, respectively. IR 140 reveals sharp features in the near-infrared spectral range around 890 nm, far away from the wavelength of excitation. Ultimately, random lasing was achieved in a solution of nanostars and styryl 14 with lasing peaks up to 973 nm, spectrally separated by 441 nm from the excitation at 532 nm.

DOI: 10.1021/acsphotonics.6b00111
ACS Photonics 2016, 3, 919–923

We note that the displayed emission intensities for the numerous random lasers are not to scale since the absorption at the excitation wavelength of 532 nm as well as the available gain differed for the respective dyes. This required diverse pump fluences (see Table 1) to overcome lasing thresholds and resulted in disparate emission intensities. Additionally, the intensities of the random lasing peaks largely fluctuated from shot to shot due to the varying arrangement of nanostars, similar to the example given in Figure 2b for pyridine 2. Control measurements for dye stock solutions without nanostars did not show distinct random lasing at the applied pump fluences, thus, ruling out feedback sources other than the nanostars. Further, a direct comparison of the random lasing behavior of gold nanostars as scattering centers to that of dielectric silicon dioxide spheres at comparable particle densities is provided in the Supporting Information, Figures S2−S4. Some intriguing aspects in regard to Figure 3 should be highlighted. As demonstrated, multimode random lasing is accomplished over 410 nm from the yellow up to the infrared spectral region. Hereby, the nanostars' broadband scattering spectra are exploited. Complex-shaped NPs, such as nanostars, exhibit multiple plasmon resonances,[24] maintaining sufficient spectral overlap with the emission of the laser dyes. Together with the huge field enhancements at their spiky tips (see, for example, Figure 3 in ref 24 and Figures 4 and 5 in ref 26), the broadband scattering of nanostars facilitates efficient random lasing over an ample range of wavelengths. Some dyes emitting at longer wavelengths, like rhodamine 800 and IR 140, tend to possess especially weak absorption cross sections at 532 nm excitation (see Table 1). Nevertheless, the illumination and detection geometry allowed us to overcome the elevated lasing thresholds even for these dyes. We note that the pump fluence for rhodamine 800 is more than twice that of IR 140 to produce the displayed random lasing spectrum, despite similarly low absorption cross sections but higher concentration than IR 140. The putative higher gain of the rhodamine 800 mixture contributes to the random lasing efficiency, but also the wavelength-dependent scattering of the nanostars. The loose minimum around 800 nm in the ensemble extinction spectrum of the nanostars (see Figure 1b) may therefore provoke a higher threshold for rhodamine 800. A lower gain could be partially compensated for by increasing the concentrations of the dye molecules in the solution. However, the concentrations were already limited by the solubility of the dyes in the particular solvent and further restricted (in our study to a few millimolar) by the addition of the nanostars in deionized water. The effect of nanoparticle concentration on random lasing in the particular case of rhodamine 6G has been previously studied.[28] A larger amount of nanostars solution also decreases the available gain; hence, a reduced concentration of nanostars was used for some dyes (see Table 1). Using DMSO instead of ethanol as solvent for the dyes emitting in the near-infrared range helped to increase the concentrations and therefore to achieve random lasing with the limited pump fluences at hand. For future improvements, Förster resonant energy transfer systems (FRET) can be envisioned as gain medium for random lasers, similar to those already used in OLEDs (Alq_3:DCM).[35] Such FRET pairs with a large Stokes shift might offer significant absorption at the excitation wavelength while revealing a stimulated emission spectrum at much higher wavelengths. However, it is noteworthy that the styryl dyes used in this study bare as well quite high absorption cross sections in the range of 1×10^{-16} cm^2 at 532 nm (see Table 1), although they emit in the deep red and infrared spectral region. It is also conspicuous that all investigated styryl dyes exhibit the most intense random lasing peaks with an almost negligible ASE background. This could be attributed to the lower reabsorption of the lasing modes due to a larger Stokes shift as compared, for example, to rhodamine 6G. Additionally, spectral coverage should be conveniently expandable even further by using an excitation laser at 400 nm (frequency-doubled Ti:Sa) or even 355 nm (frequency-tripled Nd:YAG) for applications in the near-UV spectral range, then using silver NPs to avoid intrinsic losses by the d-band absorption of gold.

In summary, we have demonstrated random lasing with immense spectral coverage facilitated by complex-shaped gold nanostars. Suspended in solutions of various laser dyes and excited at a fixed excitation wavelength, coherent lasing emission was achieved over more than 410 nm throughout the visible up to the infrared range. The efficient feedback mechanism for random lasing is attributed to the huge plasmonic hotspots at the spiky tips of the nanostars and the fact that each nanostar serves as broadband scattering center, spectrally covering the emission of a broad range of dyes.

■ ASSOCIATED CONTENT

Supporting Information

The Supporting Information is available free of charge on the ACS Publications website at DOI: 10.1021/acsphotonics.6b00111.

Cross sections from numerical calculations of a gold nanostar and a dielectric silicon dioxide nanoparticle, emission spectra of random lasers containing plasmonic nanostars and random lasers containing dielectric nanoparticles at various pump fluences (PDF).

■ AUTHOR INFORMATION

Corresponding Author

*E-mail: johannes.ziegler@jku.at.

Notes

The authors declare no competing financial interest.

■ ACKNOWLEDGMENTS

We thank H. Piglmayer-Brezina for technical support. Financial support was provided by the European Research Council within the FP7 Program via the Starting Grant 257158 "ActiveNP".

■ REFERENCES

(1) Ambartsumyan, R. V.; Basov, N. G.; Kryukov, P. G.; Letokhov, V. S. 5A10 (b)-a Laser with a Nonresonant Feedback. *IEEE J. Quantum Electron.* **1966**, *2*, 442−446.

(2) Letokhov, V. S. Generation of light by a scattering medium with negative resonance absorption. *Sov. Phys. - JETP* **1967**, *53*, 1442−1452.

(3) Lawandy, N. M.; Balachandran, R. M.; Gomes, A. S. L.; Sauvain, E. Laser Action in Strongly Scattering Media. *Nature* **1994**, *368*, 436−438.

(4) Cao, H.; Zhao, Y. G.; Ho, S. T.; Seelig, E. W.; Wang, Q. H.; Chang, R. P. H. Random Laser Action in Semiconductor Powder. *Phys. Rev. Lett.* **1999**, *82*, 2278.

(5) Frolov, S. V.; Vardeny, Z. V.; Yoshino, K.; Zakhidov, A.; Baughman, R. H. Stimulated Emission in High-Gain Organic Media. *Phys. Rev. B: Condens. Matter Mater. Phys.* **1999**, *59*, R5284.

(6) Jiang, X.; Soukoulis, C. M. Time Dependent Theory for Random Lasers. *Phys. Rev. Lett.* **2000**, *85*, 70−73.

DOI: 10.1021/acsphotonics.6b00111
ACS Photonics 2016, 3, 919−923

(7) Apalkov, V. M.; Raikh, M. E.; Shapiro, B. Random Resonators and Prelocalized Modes in Disordered Dielectric Films. *Phys. Rev. Lett.* **2002**, *89*, 016802.
(8) Vanneste, C.; Sebbah, P.; Cao, H. Lasing with Resonant Feedback in Weakly Scattering Random Systems. *Phys. Rev. Lett.* **2007**, *98*, 143902.
(9) Zaitsev, O.; Deych, L. Recent Developments in the Theory of Multimode Random Lasers. *J. Opt.* **2010**, *12*, 024001.
(10) Redding, B.; Choma, M. A.; Cao, H. Speckle-Free Laser Imaging Using Random Laser Illumination. *Nat. Photonics* **2012**, *6*, 355−359.
(11) Polson, R. C.; Vardeny, Z. V. Random Lasing in Human Tissues. *Appl. Phys. Lett.* **2004**, *85*, 1289.
(12) Wiersma, D. S. The Physics and Applications of Random Lasers. *Nat. Phys.* **2008**, *4*, 359−367.
(13) Song, Q.; Xiao, S.; Xu, Z.; Liu, J.; Sun, X.; Drachev, V.; Shalaev, V. M.; Akkus, O.; Kim, Y. L. Random Lasing in Bone Tissue. *Opt. Lett.* **2010**, *35*, 1425.
(14) Smuk, A.; Lazaro, E.; Olson, L. P.; Lawandy, N. M. Random Laser Action in Bovine Semen. *Opt. Commun.* **2011**, *284*, 1257−1258.
(15) Gottardo, S.; Cavalieri, S.; Yaroshchuk, O.; Wiersma, D. S. Quasi-Two-Dimensional Diffusive Random Laser Action. *Phys. Rev. Lett.* **2004**, *93*, 263901.
(16) Schäfer, F. P. ORGANIC DYE SOLUTION LASER. *Appl. Phys. Lett.* **1966**, *9*, 306.
(17) Dulkeith, E.; Morteani, A. C.; Niedereichholz, T.; Klar, T. A.; Feldmann, J.; Levi, S. A.; van Veggel, F. C. J. M.; Reinhoudt, D. N.; Möller, M.; Gittins, D. I. Fluorescence Quenching of Dye Molecules near Gold Nanoparticles: Radiative and Nonradiative Effects. *Phys. Rev. Lett.* **2002**, *89*, 203002.
(18) Khatua, S.; Paulo, P. M. R.; Yuan, H.; Gupta, A.; Zijlstra, P.; Orrit, M. Resonant Plasmonic Enhancement of Single-Molecule Fluorescence by Individual Gold Nanorods. *ACS Nano* **2014**, *8*, 4440−4449.
(19) Barbosa, S.; Agrawal, A.; Rodríguez-Lorenzo, L.; Pastoriza-Santos, I.; Alvarez-Puebla, R. A.; Kornowski, A.; Weller, H.; Liz-Marzán, L. M. Tuning Size and Sensing Properties in Colloidal Gold Nanostars. *Langmuir* **2010**, *26*, 14943−14950.
(20) Le Ru, E. C.; Grand, J.; Sow, I.; Somerville, W. R. C.; Etchegoin, P. G.; Treguer-Delapierre, M.; Charron, G.; Félidj, N.; Lévi, G.; Aubard, J. A Scheme for Detecting Every Single Target Molecule with Surface-Enhanced Raman Spectroscopy. *Nano Lett.* **2011**, *11*, 5013−5019.
(21) Sau, T. K.; Rogach, A. L. *Complex-Shaped Metal Nanoparticles: Bottom-Up Syntheses and Applications*; Wiley-VCH: Weinheim, Germany, 2012.
(22) Loumaigne, M.; Navarro, J. R. G.; Parola, S.; Werts, M. H. V.; Débarre, A. The Intrinsic Luminescence of Individual Plasmonic Nanostructures in Aqueous Suspension by Photon Time-of-Flight Spectroscopy. *Nanoscale* **2015**, *7*, 9013−9024.
(23) Gollner, C.; Ziegler, J.; Protesescu, L.; Dirin, D. N.; Lechner, R. T.; Fritz-Popovski, G.; Sytnyk, M.; Yakunin, S.; Rotter, S.; Yousefi Amin, A. A.; Vidal, C.; Hrelescu, C.; Klar, T. A.; Kovalenko, M. V.; Heiss, W. Random Lasing with Systematic Threshold Behavior in Films of CdSe/CdS Core/Thick-Shell Colloidal Quantum Dots. *ACS Nano* **2015**, *9*, 9792−9801.
(24) Hao, F.; Nehl, C. L.; Hafner, J. H.; Nordlander, P. Plasmon Resonances of a Gold Nanostar. *Nano Lett.* **2007**, *7*, 729−732.
(25) Hrelescu, C.; Sau, T. K.; Rogach, A. L.; Jäckel, F.; Laurent, G.; Douillard, L.; Charra, F. Selective Excitation of Individual Plasmonic Hotspots at the Tips of Single Gold Nanostars. *Nano Lett.* **2011**, *11*, 402−407.
(26) Perassi, E. M.; Hrelescu, C.; Wisnet, A.; Döblinger, M.; Scheu, C.; Jäckel, F.; Coronado, E. A.; Feldmann, J. Quantitative Understanding of the Optical Properties of a Single, Complex-Shaped Gold Nanoparticle from Experiment and Theory. *ACS Nano* **2014**, *8*, 4395−4402.
(27) Hrelescu, C.; Sau, T. K.; Rogach, A. L.; Jackel, F.; Feldmann, J. Single Gold Nanostars Enhance Raman Scattering. *Appl. Phys. Lett.* **2009**, *94*, 153113.
(28) Dice, G. D.; Mujumdar, S.; Elezzabi, A. Y. Plasmonically Enhanced Diffusive and Subdiffusive Metal Nanoparticle-Dye Random Laser. *Appl. Phys. Lett.* **2005**, *86*, 131105.
(29) Popov, O.; Zilbershtein, A.; Davidov, D. Random Lasing from Dye-Gold Nanoparticles in Polymer Films: Enhanced Gain at the Surface-Plasmon-Resonance Wavelength. *Appl. Phys. Lett.* **2006**, *89*, 191116.
(30) Zhai, T.; Zhang, X.; Pang, Z.; Su, X.; Liu, H.; Feng, S.; Wang, L. Random Laser Based on Waveguided Plasmonic Gain Channels. *Nano Lett.* **2011**, *11*, 4295−4298.
(31) Heydari, E.; Flehr, R.; Stumpe, J. Influence of Spacer Layer on Enhancement of Nanoplasmon-Assisted Random Lasing. *Appl. Phys. Lett.* **2013**, *102*, 133110.
(32) Meng, X.; Fujita, K.; Moriguchi, Y.; Zong, Y.; Tanaka, K. Metal-Dielectric Core-Shell Nanoparticles: Advanced Plasmonic Architectures Towards Multiple Control of Random Lasers. *Adv. Opt. Mater.* **2013**, *1*, 573−580.
(33) Meng, X.; Fujita, K.; Zong, Y.; Murai, S.; Tanaka, K. Random Lasers with Coherent Feedback from Highly Transparent Polymer Films Embedded with Silver Nanoparticles. *Appl. Phys. Lett.* **2008**, *92*, 201112.
(34) Meng, X.; Fujita, K.; Murai, S.; Matoba, T.; Tanaka, K. Plasmonically Controlled Lasing Resonance with Metallic−Dielectric Core−Shell Nanoparticles. *Nano Lett.* **2011**, *11*, 1374−1378.
(35) Kozlov, V. G.; Bulović, V.; Burrows, P. E.; Forrest, S. R. Laser Action in Organic Semiconductor Waveguide and Double-Heterostructure Devices. *Nature* **1997**, *389*, 362−364.
(36) Berggren, A.; Dodabalapur, A.; Slusher, R. E.; Bao, Z. Light Amplification in Organic Thin Films Using Cascade Energy Transfer. *Nature* **1997**, *389*, 466−469.
(37) Cerdán, L.; Enciso, E.; Martín, V.; Bañuelos, J.; López-Arbeloa, I.; Costela, A.; García-Moreno, I. FRET-Assisted Laser Emission in Colloidal Suspensions of Dye-Doped Latex Nanoparticles. *Nat. Photonics* **2012**, *6*, 621−626.
(38) Cao, H.; Zhao, Y. G.; Ong, H. C.; Ho, S. T.; Dai, J. Y.; Wu, J. Y.; Chang, R. P. H. Ultraviolet Lasing in Resonators Formed by Scattering in Semiconductor Polycrystalline Films. *Appl. Phys. Lett.* **1998**, *73*, 3656.
(39) Markushev, V. M.; Zolin, V. F.; Briskina, C. M. Luminescence and Stimulated Emission of Neodymium in Sodium Lanthanum Molybdate Powders. *Sov. J. Quantum Electron.* **1986**, *16*, 281.
(40) Azkargorta, J.; Bettinelli, M.; Iparraguirre, I.; Garcia-Revilla, S.; Balda, R.; Fernández, J. Random Lasing in Nd:LuVO_4 Crystal Powder. *Opt. Express* **2011**, *19*, 19591.
(41) Liang, H. K.; Meng, B.; Liang, G.; Tao, J.; Chong, Y.; Wang, Q. J.; Zhang, Y. Electrically Pumped Mid-Infrared Random Lasers. *Adv. Mater.* **2013**, *25*, 6859−6863.
(42) Ziegler, J.; Djiango, M.; Vidal, C.; Hrelescu, C.; Klar, T. A. Gold Nanostars for Random Lasing Enhancement. *Opt. Express* **2015**, *23*, 15152.
(43) Liu; Guyot-Sionnest, P. Mechanism of Silver(I)-Assisted Growth of Gold Nanorods and Bipyramids. *J. Phys. Chem. B* **2005**, *109*, 22192−22200.
(44) Brackmann, U. *Lambdachrome Laser Dyes: Data Sheets*, 3rd ed.; Lambda Physik: Göttingen, Germany, 2000.
(45) Meng, X.; Kildishev, A. V.; Fujita, K.; Tanaka, K.; Shalaev, V. M. Wavelength-Tunable Spasing in the Visible. *Nano Lett.* **2013**, *13*, 4106−4112.

DOI: 10.1021/acsphotonics.6b00111
ACS Photonics 2016, 3, 919−923